Low-Fouling Amine-Terminated Poly(ethylene glycol) Thin Layers and Effect of Immobilization Conditions on Their Mechanical and Physicochemical Properties

Yves Martin[†,‡] and Patrick Vermette*[,†,‡]

Department of Chemical Engineering, Université de Sherbrooke, 2500, blvd de l'Université, Sherbrooke, Québec, Canada J1K 2R1, and Research Centre for Aging, Institut universitaire de gériatrie de Sherbrooke, 1036, rue Belvédère Sud, Sherbrooke, Québec, Canada J1H 4C4

Received April 26, 2006; Revised Manuscript Received September 1, 2006

ABSTRACT: The physicochemical and mechanical properties of amine-terminated covalently bound poly(ethylene glycol) (PEG) layers are dependent on fabrication methods. In particular, the use of a Θ solvent yields dense polymer layers with properties not well described by traditional models. Light diffraction techniques were used in an attempt to understand the influence of polymer aggregation kinetics in a Θ solvent on the final properties of the fabricated PEG layers. The polymer layer properties were characterized using X-ray photoelectron spectroscopy (XPS), atomic force microscopy (AFM) in force mode, quartz crystal microbalance (QCM), and fluorescence microscopy. Results show that polymer concentration in solution is an important indicator of final layer properties and that the use of a Θ solvent induces complex aggregation phenomena in solution yielding layers with widely different properties. The PEG layers fabricated through the process described in this article are also shown to present chemically available primary amine groups, paving the way for the immobilization of bioactive molecules.

1. Introduction

Poly(ethylene glycol)-modified (PEG-modified) surfaces have attracted much attention in the past years due to their good anti-biofouling properties. PEG-coated surfaces are reported to exhibit their anti-biofouling potential mainly through their resistance to nonspecific protein adsorption. However, it is not yet clear what forces predominantly come into play to repel proteins from adhering to varyingly ordered hydrated PEG layers. Atomic force microscopy (AFM) and surface force apparatus (SFA) studies have yielded partial answers, namely that steric repulsion and/or hydration/water structuring interactions are mainly responsible for this capacity. Other types of interactions that must be reported when attempting to model PEG layers resistance toward protein adsorption include electrical double-layer interactions and van der Waals interactions, both of which can be attractive forces. PEG layers thus generally provide a repulsive interaction barrier through steric repulsion and hydration/water structuring of greater magnitude and longer range than either attractive electrostatic or van der Waals interactions.[1] The importance of the repulsive interaction barrier, which is directly proportional to the resistance to protein adhesion, is dependent on the exact structure of immobilized PEG layers. From the well-known theories of de Gennes and Alexander,[2,3] in which the conformation of grafted polymers is dependent on the radius of gyration of the polymer, the distance between grafting points and the quality of the solvent, so-called "brush", "mushroom", and "pancake" conformations are described. The "brush" conformation represents tightly packed and extended polymer chains while the "pancake" represents rather flat and noninteracting polymer chains, and the "mushroom" stands somewhere in the middle of the two preceding conformations (more or less tightly gathered polymer "balls"). It is widely believed that brush conformations, where the polymer chains are the most tightly crowded on the surface, yield the highest energy barrier to protein adsorption. This is, however, subject to caution as a study on self-assembled monolayers of ethylene oxide-terminated molecules showed that very high ethylene oxide densities can enhance protein adsorption by varying chain conformation and water structuring characteristics.[4]

Different approaches can be undertaken to graft PEG molecules densely on surfaces in a "brush" conformation to minimize protein adsorption. Modified PEG molecules can be either adsorbed on a substrate or covalently immobilized. PEG-covered surfaces produced using simple physisorption can detach, as has been observed in some studies for poly(lysine)−PEG surfaces.[5] It is believed that to achieve stable high-density PEG layers, covalent immobilization is preferable to simple adsorption. Moreover, the PEG molecular weight, its concentration in solution, the use of branched polymers, the nature of the solvent used for immobilization, and the number of grafting sites on the substrate all contribute to yield different immobilized PEG layers. Thus, many reports have been published to study the effect of these parameters on final layer conformation.[5−10] Although a complete picture has not yet been developed, it is clear that the use of a Θ solvent or of a poor solvent yields layers of substantially higher polymer density and enhanced low-fouling properties as first reported by Golander et al.[11] and subsequently by others.[12,13] High-density coatings obtained by covalent grafting from a good solvent are difficult to achieve due to the steric hindrance of PEG chains as they approach a surface which already contains some grafted chains. This effect can be lessened by carrying out the PEG conjugation to the solid support at or just slightly below the cloud point temperature, where the intrachain segment repulsions are small.

Although numerous reports have been published on the fabrication and characterization of PEG layers, a much smaller number have been written on the application of specific PEG as a base material for modulating specific cell responses. For

† Université de Sherbrooke.
‡ Institut universitaire de gériatrie de Sherbrooke.
* Corresponding author: Ph 1-819-821-8000 ext 62826; Fax 1-819-821-7955; e-mail Patrick.Vermette@USherbrooke.ca.

10.1021/ma060921f CCC: $33.50
Published on Web 10/17/2006

example, one interesting application, in our opinion, is the use of terminally modified PEG layers to allow subsequent covalent addition of bioactive molecules. Such systems, although not widely described in the literature, have been reported in efforts to minimize nonspecific binding of biological compounds (e.g., proteins) in label-free monitoring of affinity interactions,[14] for the in-vitro control of cellular attachment and proliferation,[15] and for the modulation of the coagulation of whole blood on PEG surfaces.[16] Considerable efforts are also made to locate geometrically bioactive compounds on low-fouling layers to achieve superior modulation of in-vitro cell behavior. The principal techniques currently available to produce such systems are described in an excellent review by Li et al.[17]

This study aimed to develop an optimized and characterized PEG-based system to allow the localized covalent binding of a variety of bioactive molecules onto a wide range of substrates. Efforts were placed to understand the effect of reaction parameters on physicochemical and mechanical hydrated PEG layer properties. Quartz crystal microbalance (QCM), atomic force microscopy (AFM) using the colloidal probe force measurement, and X-ray photoelectron spectroscopy (XPS) were used to achieve this understanding critical for cell-based applications. The PEG layers produced in Θ solvents were found to show important discrepancies to traditional models, and further investigation was carried out to assess the possible effect of polymer aggregate kinetics in solution at different polymer concentrations on PEG layer properties. The measure of aggregate sizes was achieved using light diffraction. To our knowledge, this is the first study to attempt to understand the significance of cloud point colloidal properties on immobilized polymer layer physicochemical and mechanical properties. Moreover, techniques originating from DNA and protein chip manufacture were also used to allow the creation of patterns of covalently bound molecules onto the PEG layers. The possibility to produce defined patterns was assessed by fluorescence techniques.

2. Experimental Section

2.1. Plasma Polymer Surfaces. Plasma-enhanced chemical vapor deposition (PECVD) was used to create stable reactive amine-bearing layers through a process previously described.[18,19] Briefly, substrates to be modified were introduced into a homemade cylindrical plasma reactor. *N*-Heptylamine monomer (Sigma, Ontario, Canada, cat. 126802) was introduced in the reactor chamber until a pressure of 40 mTorr was reached. The PECVD process was initiated by applying a radio-frequency current between two electrodes. The samples were deposited onto the bottom electrode. The operating conditions were set at a frequency of 50 kHz, a glow discharge power of 80 W, a distance between the electrodes of 10 cm, and a deposition time of 45 s. The choice of the operating conditions was based on a previous study aiming to maximize the quantity of surface reactive amines and to obtain layers of 25 nm (to be published).

2.2. PEG Layer Fabrication. Heptylamine plasma polymer (HApp) substrates were made to react at room temperature in a solution of Boc-NH_2-poly(ethylene glycol)-NHS of 3400 Da molecular weight from Nektar Therapeutics (San Carlos, CA, cat. 4M530F02). The PEG concentration was varied from 0.1 to 5 mg/mL in either deionized water or a Θ solvent, in this case a Na_2SO_4 solution near saturation (Sigma, Ontario, Canada, cat. 239313). Cloud point formation was used to define the Θ solvent, which was not previously known for this polymer at room temperature. It should be noted that the cloud point phenomenon occurs in a slightly poorer solvent than the actual Θ solvent. Samples were allowed to react overnight under agitation and rinsed repeatedly in saline solutions and deionized water to remove salts and unbound PEG molecules. Varied substrates were used to immobilize the PEG layers depending on end use. Perfluorinated poly(ethylene-*co*-propylene) tape from Dupont (Teflon FEP Type A, Mississauga, Canada) was used for XPS analyses and fluorescence studies. This substrate was chosen mainly for its ease of use and the possibility to detect a fluorine signal in XPS analyses. Quartz substrates coated with gold electrodes for QCM analyses were bought from Maxtek (CA, 5 MHz blanks). Cleaved mica substrates were used for AFM force measurements. All substrates were cleaned in RBS 35 surfactant (Pierce, Rockford, IL, cat. 27952), rinsed in water and in ethanol, and blown-dried using filtered air. Immobilized Boc-NH_2-PEG-plasma layers were Boc-deprotected following manufacturer's recommendations by immersing the substrates in a 50% v/v solution of trifluoroacetic acid (Sigma, Ontario, Canada, cat. T62200) and dichloromethane (Sigma, Ontario, Canada, cat. D65100) for 1 h. The substrates were afterward repeatedly rinsed in a 5% v/v solution of *N*,*N*-diisopropylethylamine (Sigma, Ontario, Canada, cat. D3887) in dichloromethane.

2.3. Surface Chemical Composition by X-ray Photoelectron Spectroscopy (XPS) Measurements. XPS analyses were performed using an AXIS HSi spectrometer from Kratos Analytical Ltd. (Manchester, UK). XPS measurements were conducted with a monochromated aluminum Kα source at a power of 180 W. The pressure of the XPS chamber during measurements was lower than 5×10^{-8} mbar. FEP samples were fixed on XPS holder by a silver glue to prevent charge accumulation during measurements. High-resolution C 1s and N 1s spectra, along with survey spectra, were taken for each sample. Moreover, at least three different areas on each substrate were analyzed. Each condition was represented by at least three samples.

2.4. Viscoelastic Properties of PEG Layers and Protein Adsorption by Quartz Crystal Microbalance (QCM) Measurements. Quartz crystal microbalance measurements were performed using an apparatus from Resonant Probes GmbH (Hochgrevestr, Germany). The gold-coated quartz resonators were placed into a commercial holder (Maxtek (CA), CHT100). Data from the network analyzer (Agilent, Palo Alto, CA, HP4396A) was analyzed using the software from Resonant Probes. For protein adsorption assays, PEG-coated substrates were placed in the QCM holder immersed in a 37 °C bath to maintain the temperature constant. RPMI 1640 medium (Sigma, Ontario, Canada, cat. R8758) at the same temperature was automatically injected at a rate of 10 mL/min into the QCM chamber. Upon stability of the signal (at least 1 h), a solution of 10% v/v decomplemented fetal bovine serum (Sigma, Ontario, Canada, cat. F2442) in RPMI 1640 was injected into the chamber at 10 mL/min. This injection was normalized at time 5 min to compare different layers. The choice of the protein medium used for the adsorption tests was dictated by the wide range of proteins contained in FBS, so that the versatility of protein resistance of the layers could be assessed. The frequency and half-band-half-width shift (i.e., the dissipation times the frequency of vibration divided by two) were recorded by the software to monitor changes in layer mass (e.g., adsorption of proteins) and in layer viscoelastic properties.

For PEG grafting monitoring (i.e., so-called PEGylation), plasma-modified QCM substrates were rapidly placed into the holder in contact with water. The frequencies of harmonic vibrations were located, and a Boc-PEG-NHS solution was automatically introduced into the holder at a rate of 10 mL/min. The frequency and half-band-half-width signals were recorded as for the adsorptions assays. In this case, the whole system was maintained at room temperature (i.e., 22 °C) for the PEGylation tests. For hydration assays, PEG layers covalently attached onto the quartz resonators were blown-dried and placed into a desiccator for at least 48 h. The crystals were placed rapidly into the dry holder, and harmonics were taken in air. Water was injected at a rate of 10 mL/min for 30 s, and variations in frequency and half-band-half-width were measured until stabilization of the signals (at least 1 h). Other water injections were made to ensure a stable signal. All QCM experiments were carried out in at least two different samples for each condition. For all QCM measurements, data were taken at least for harmonics located at 15, 25, 35, and 45 MHz (the fundamental frequency being

Table 1. XPS Survey Data for Different PEG-Treated Samples[a]

sample	% C	% O	% N	% F	O/C	N/C	exposure to oxygen
FEP	35.8 ± 0.6	0.9 ± 0.2	0.0	63 ± 1	0.03	0.00	NA
heptylamine plasma	87 ± 1	2.5 ± 0.5	10.1 ± 0.5	0.0	0.03	0.12	<30 min
heptylamine plasma	83.4 ± 0.8	9.3 ± 0.5	7.3 ± 0.5	0.0	0.11	0.09	>3 days
PEG 0.1 mg/mL	81 ± 1	13.0 ± 0.4	5.4 ± 0.2	0.0	0.16	0.07	>3 days
PEG 1 mg/mL	81 ± 1	13 ± 2	5.3 ± 0.4	0.0	0.16	0.07	>3 days
PEG 5 mg/mL	81 ± 1	12.6 ± 0.6	6.1 ± 0.4	0.0	0.16	0.08	>3 days
PEG 0.1 mg/mL CP	81.4 ± 0.5	14.0 ± 0.5	4.6 ± 0.2	0.0	0.17	0.06	>3 days
PEG 1 mg/mL CP	77 ± 1	18.6 ± 0.8	4.5 ± 0.3	0.0	0.24	0.06	>3 days
PEG 5 mg/mL CP	79 ± 1	15.7 ± 0.9	5.3 ± 0.5	0.0	0.20	0.07	>3 days

[a] CP is used in the table to denote samples fabricated from a PEG solution in a cloud point state.

5 MHz). Harmonic number 5 (i.e., 25 MHz) is the harmonic reported in the graphics of this article.

2.5. PEG Layers Structure by Atomic Force Microscopy (AFM) Force Measurements. A Bioscope (Digital Instruments, Santa Barbara, CA) coupled to a Zeiss inverted microscope and linked to a Nanoscope IIIa controller was used to conduct force measurements on the hydrated PEG layers based on the colloidal probe method as previously described.[20] Briefly, the AFM was operated at a frequency of 1 Hz and ramp sizes of 100, 250, and 500 nm, recording both approaching and extending data. Silica microspheres of 4.12 μm of diameter (Bangs Laboratories, Fisher, IN, cat. SS05N) were attached using medical-grade epoxy-type glue (Master Bond, Hackensack, NJ, cat. EP30MED) to Si_3N_4 cantilevers with a measured spring constant of 0.137 N/m (Veeco, Woodbury, NY, DNP-S) using the resonance method proposed by Cleveland et al.[21] Cantilever deflection and *z*-piezo position were transformed into force vs distance curves using a homemade software based on the developments by Ducker et al.[22] This software is made freely available upon request to P. Vermette. Force measures were done at room temperature in 100, 10, and 1 mOsm NaCl solutions buffered in 10 mM Hepes, in RPMI 1640 media, and in deionized water, allowing for at least 1 h of stabilization before taking measures. At least three different spots were studied on each sample, and at least 20 force curves were recorded for each spot.

2.6. PEG Aggregation Measurements during Cloud Point Conditions. While in a slightly poorer solvent than the Θ solvent, the Boc-PEG-NHS polymer forms aggregates that are visible to the naked eye through the formation of cloudiness in the solution (thus the term "cloud point"). A Malvern Mastersizer 2000 (Malvern Instruments, Malvern, UK) was used to measure the aggregate size distribution based on the light diffraction technique (i.e., aggregates yield different diffraction patterns relative to their size). The particle size was determined as a function of time using a measured refractive index for the solvent of 1.35787 (using a refractometer from Schmidt + Haensch, model DUR-W2, GER) and a refractive index of 1.47 for the PEG aggregates.[9] The approximate shear rate during the measures was 34 s^{-1}, corresponding to a stirring rate of 150 rpm.[23] The instrument was thoroughly cleaned before each sample. The solvent was first introduced into the circulation loop of the apparatus. A concentrated homogenized PEG solution was fabricated by hand agitation and rapidly added at time 0 min into the circulation loop of the apparatus to achieve the desired final PEG concentration. This procedure contrasts with other procedures reported to monitor PEG agglomeration in Θ solvent where the PEG is completely dissolved in a good solvent such as water before incorporation in the apparatus filled with the Θ solvent.[23] The procedure was chosen to mimic the actual use of the PEG molecules to form layers as speed is necessary to avoid hydrolysis of the active ester end group before exposure to the amine substrate.

2.7. Chemical Bonding of Carboxyfluorescein to the Amine-Bearing PEG Surfaces. A BioChip Arrayer (PerkinElmer, Wellesley, MA) was used to dispense picoliters of solution to precise locations on PEG surfaces. Carboxyfluorescein (CF, Molecular Probes, Eugene, OR, cat. C-194) was made to react with the deprotected amine groups on the PEG layers through the use of *N*-ethyl-*N*′-(3-(dimethylamino)propyl)carbodiimide (EDC) (Sigma, Ontario, Canada, cat. E1769) and *N*-hydroxysuccinimide (NHS) (Sigma, Ontario, Canada, cat. H7377) to form a stable amide bond between the PEG layer and the fluorescent molecules. Solutions with ratios of 0.5:0.5:1 between EDC:NHS:CF using different CF concentrations were placed in multiwell plates. The Biochip Arrayer sampled the solutions to deposit droplets of ca. 300 pL at different locations on the substrates, in this case to form the layer "Y" with dots varyingly spaced. One or both of the activated carboxylic groups on the CF molecule could then react with the amine groups available on the PEG-coated substrates and form stable amide bonds. Samples were then rinsed thoroughly in saline buffer and in deionized water while avoiding exposure to light. Fluorescence was preserved by using FluoroGuard (Bio-Rad Laboratories, Hercules, CA) and fixing the FEP samples beneath a glass coverslip with transparent nail polish. Fluorescence on the samples was observed using a Leica binocular microscope with appropriate filters. Photos were taken at an exposure of 1 s, and green intensity was measured using SigmaScan Pro software (Systat Software, Richmond, CA). Calibration curves were constructed to ensure the use of proper concentrations of CF to deposit on the surfaces to be in a linear regime and avoid quenching. CF solutions of concentrations ranging from 0.017 to 1.7 mM were thus made to react with three different samples. For each sample, it was observed that the use of a 0.17 mM CF solution was in a linear and nonquenching regime (data not shown), and this concentration was then deposited on all samples to be tested. At least 20 droplets were deposited on each sample, and at least two samples were studied for each immobilization condition.

3. Results and Discussion

3.1. Chemical Properties of the PEG Layers. Covalent immobilization of protected Boc-PEG-NHS onto radio-frequency generated plasma reactive amine layer was performed at PEG solution concentrations varying from 0.1 to 5 mg/mL in either water or an aqueous Na_2SO_4 Θ solvent (yielding the so-called cloud point or CP condition). Successful covalent immobilization of the polymer layers can be monitored by XPS measurements. Table 1 presents the atomic composition of different PEG layers obtained from XPS survey spectra.

From data of Table 1 and Figure 1, it is clear that the use of the Θ solvent increases the amount of PEG molecules immobilized on the surface, as was previously reported for other systems.[11,12] The observed oxygen present on all PEG-treated surfaces increases markedly compared to the oxidized bare plasma layer. This effect, however, is much more important for surfaces where the polymer was immobilized under cloud point conditions, with a maximum O/C ratio of 0.24 observed for the 1 mg/mL case. Considering the molecular formula, a pure PEG layer would present an O/C ratio of close to 0.33. Such a high ratio would be very surprising in a nonhydrated environment (even for a brushlike structure that can be adopted by the PEG layers), such as in the XPS chamber, where the PEG chains known to be surrounded by water molecules in an aqueous environment probably collapse when dried and yield layers thinner than 10 nm (i.e., the depth of analysis of the XPS instrument). It is worthy to notice that the highest O/C ratio does not come from the highest PEG solution concentration, 5

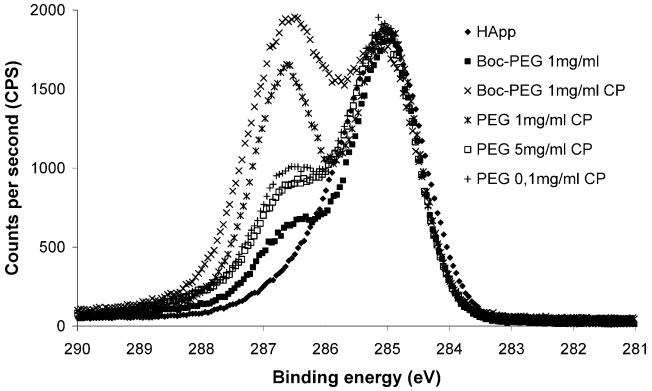

Figure 1. XPS C 1s high-resolution spectra of different PEG-covered samples.

mg/mL, but from the intermediate concentration of 1 mg/mL. More than XPS data is needed to understand the phenomenon.

Table 1 also indicates that the surface chemical composition of PEG layers deposited under good solvent conditions (i.e., non-cloud point) is not affected by the PEG concentration; i.e., changing the solution concentration of the polymer did not significantly modify the O/C ratio for these layers.

The experimental error on atomic composition, while not relatively large for most samples, is important for oxidized plasma samples. This is attributed to the difference in the time elapsed between the fabrication of the samples and the XPS analyses of the different samples.

Although a high O/C ratio can indicate the presence of the characteristic repeating ether chemical bonds of the PEG molecule, it is impossible to distinguish contributions from other oxygen sources such as the oxidation results of the base plasma layer. High-resolution carbon spectra can then be used to identify the nature of carbon bonds on the surface. Such spectra of the different samples are presented in Figure 1.

By comparing the oxidized heptylamine plasma layer (HApp) of Figure 1 to the immobilized PEG layers, it is clear that the ether carbon (located at 286.5 eV) is more important for layers with PEG and that the proportions of Table 1 are respected. High-resolution nitrogen spectra were also recorded to ensure that C−N bonds (also located at 286.5 eV) are not responsible for the different intensities (data not shown).

XPS data were also used to confirm the stability of the PEG layers both after autoclaving and after acidic Boc deprotection using trifluoroacetic acid (data not shown). The absence of contaminants such as salts and silicone was also verified. As observed in Table 1, no samples present Fluor atoms except for the bare FEP tape. This indicates that the plasma layer is thicker than the depth of analysis of the instrument estimated at ca. 10 nm, and no "holes" were detected (by AFM imaging) in the substrates.

The results presented in Table 1 and Figure 1, although indicative of the quantity of PEG molecules covalently immobilized on heptylamine plasma polymer-coated (HApp-coated) FEP surfaces, do not give information on the architecture of the hydrated layers and can be misleading when attempting to correlate results with future biological responses. Thus, measurements in aqueous environments are mandatory to assess the real impact of immobilization methods on layer architecture.

3.2. PEG Layer Resistance to Protein Adsorption. The main reason to produce substrates covered by thin PEG layers is to lower or eliminate nonspecific cell−material interactions. A good estimation of this property is to monitor dynamic protein adsorption on the polymer layers, as this adsorption will dictate the interaction level of cells with the material. The quartz crystal microbalance apparatus (QCM) was used to measure the adsorption of the large spectra of proteins found in fetal bovine serum (FBS) on the different PEG samples. This can be accomplished with the QCM through the analysis of the frequency and half-band-half-width (HBHW) signals, as the QCM apparatus directly measures minute changes in the distribution of oscillating frequencies of a gold-coated quartz crystal occurring as the load present on the crystal changes. Among the advantages of the technique is the possibility to work in different aqueous media and the extreme sensitivity of the technique. The results for protein adsorption are shown in Table 2.

The lowering of the resonance frequency of the vibrating quartz crystal in QCM experiments is physically correlated with the mass of material vibrating with the crystal. For systems where no energy loss is associated with the vibration, the variation in frequency is proportional to the mass on the crystal through the well-known Sauerbrey equation. However, for the protein-containing aqueous system used in this study, vibration energy losses are present, and thus, the Sauerbrey mass is only an approximation of the real protein mass adsorbed on the crystal.

From Table 2, while gold and plasma layers adsorb equivalent quantities of protein from FBS, large differences are observed for PEG-treated samples. PEG surfaces obtained from non-cloud point conditions were all shown to adsorb significant amount of proteins; the best and worst surfaces are listed in Table 2. While no significant variations in chemistry was apparent by XPS measurements, higher PEG concentrations are shown to achieve superior protein repellency properties. In this case, a solution of 5 mg/mL PEG lowers approximately by half the amount of adsorbed proteins by bare gold, plasma, or 0.1 mg/mL PEG surfaces assuming similar energy losses in all systems.

Once again, the effect of using a Θ solvent for immobilization is significant as PEG samples made using 1−5 mg/mL of PEG in Θ solvent conditions almost completely repel protein adsorption. Samples produced using 5 mg/mL PEG solutions under cloud point conditions lower protein adsorption below the threshold of the sensitivity of the technique. For the PEG surfaces under study (i.e., hydrated viscoelastic layers), the sensitivity of the QCM apparatus is in the 2 Hz range, as determined by the standard deviations obtained from different steady-state measurements. This result is coherent, to some extent, to the XPS data, where maximal PEG molecules were immobilized for these two conditions, although the 1 mg/mL PEG sample (under cloud point), which was shown to present more PEG molecules, adsorbs slightly (but significantly) more proteins on its surface. Perhaps in this case an effect of the architecture of the PEG molecules comes into play, where too densely packed EO change conformation, losing some water binding capabilities, and become more prone to protein adsorption as previously reported for self-assembled monolayers.[4] PEG samples produced using 0.1 mg/mL (under cloud point) show a particular response to protein adsorption, as proteins seem to be able to adsorb on the surface in much larger amounts than on control surfaces (i.e., gold and plasma layers). Again, it seems very likely that the architecture of the polymers on the surface plays a large role in this phenomenon. It should also be recalled that this PEG sample (0.1 mg/mL CP) presents a larger number of molecules on its surface than surfaces produced under non-cloud point conditions as shown by XPS data, and as such, it is surprising to note its protein "trapping" behavior. An intermediate concentration of 0.5 mg/mL was also tested, yielding superior

Table 2. QCM Results Presenting Protein Adsorption on Different PEG-Coated Quartz Crystals at Steady State[a]

surface	av freq shift (Hz)	Sauerbrey protein mass (ng/mm^2)	av half-band-half-width shift	time to steady state (min)
gold	-270 ± 6	0.95 ± 0.02	75 ± 5	2 ± 1
heptylamine plasma	-291 ± 8	1.03 ± 0.03	80 ± 10	18 ± 1
PEG 0.1 mg/mL CP	-560 ± 30	2.0 ± 0.1	200 ± 30	30 ± 1
PEG 0.5 mg/mL CP	-215 ± 6	0.8 ± 0.2	75 ± 6	10 ± 1
PEG 1 mg/mL CP	-11 ± 3	0.1 ± 0.1	0	13 ± 1
PEG 1 mg/mL CP (deprotected)	-48 ± 5	0.2 ± 0.2	52 ± 8	20 ± 1
PEG 5 mg/mL CP	0	0	0	5 ± 1
PEG 5 mg/mL	-150 ± 10	0.53 ± 0.04	25 ± 4	3 ± 1
PEG 0.1 mg/mL	-290 ± 10	1.00 ± 0.04	88 ± 6	3 ± 1

[a] CP is used to denote samples fabricated from a PEG solution in a cloud point state.

protein repellency than the gold and HApp control surfaces, but much poorer than 1 and 5 mg/mL PEG surfaces produced under cloud point conditions.

One final aspect to be noted is that Boc deprotection increases slightly the amount of adsorbed protein at steady state. This effect was predicted as deprotected sample present a positively charged terminal amine group, which can create electrostatic forces of significance with negatively charged protein domains. However, this effect is marginal for most surfaces (the worst case being presented in Table 2) and is proportional to the amount (by XPS) of PEG present on the surface (i.e., sample 1 mg/mL presents the larger number of PEG molecules and thus would present the larger electrostatic effect).

The property of PEG layers to resist protein adsorption is, as previously mentioned, attributed mainly to high steric repulsion forces and water structuring/hydration forces.[1] High steric forces are traditionally associated with brushlike structures and dense PEG coatings. However, from the QCM data of Table 2 and XPS results of Table 1, dense PEG layers do not necessarily translate into higher anti-biofouling properties, noticeably for PEG samples produced using 1 and 0.1 mg/mL (under cloud point conditions). Then, water structuring/hydration forces are probably responsible for part of the observed behavior of the layers to protein adsorption.

To get a better insight into the water structuring properties of the different samples, QCM hydration measurements were made where water was rapidly injected on dried PEG layers and frequency and half-band-half-width signals were recorded. These results are presented in Figure 2.

Figure 2 presents the hydration data of four representative PEG surfaces. The samples that were not constructed using cloud point conditions present similar dynamic behaviors, rapidly (i.e., less than 1 min) reaching a steady state and show comparable frequency and half-band-half-width shifts. This indicates similar water uptake and water structuring properties. However, surfaces constructed with the use of a Θ solvent present important differences between samples. First, surfaces covered with 0.1 mg/mL PEG (under cloud point) were shown to entrap more water molecules than all other samples illustrated by a 33% decreased frequency shift and a 70% increased half-band-half-width (compared to the other three PEG surfaces tested). Moreover, this water is rapidly arranged around the PEG molecules as the steady state of the system is also reached in less than 1 min. Second, the sample constructed with 5 mg/mL PEG (under cloud point) reaches similar frequency and half-band-half-width shifts than non-cloud point samples but shows a different dynamic behavior.

In control theory, physical systems dynamic responses to stimuli can be expressed either as first-, second-, or higher-order differential equations, depending on the physical phenomena. From this observation, variables can be used to

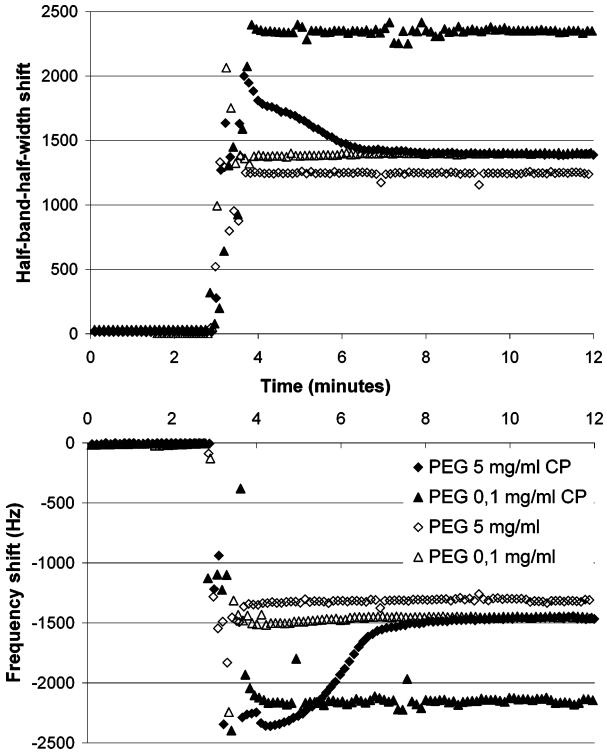

Figure 2. QCM hydration data of four PEG-covered surfaces with water injection at 3 min.

completely define dynamic responses; for second-order systems, three variables are sufficient. They are the steady-state gain (i.e., K_p in the standard nomenclature of second-order systems), which basically gives the steady-state variation between unperturbed and perturbed states, the natural period of oscillation (i.e., τ), and the damping factor (i.e., ζ) which together express the dynamic "shape" of the response. In Figure 2, PEG surfaces made with 5 mg/mL (under cloud point) present a second-order dynamic behavior relative to the frequency shift as illustrated by the "S" shape of the system frequency response to hydration (i.e., there is an initial lag in the frequency response). A similar dynamic behavior is observed for samples made with 1 mg/mL (under cloud point) (data not shown). While the steady-state gains (i.e., the K_p) of the 1 and 5 mg/mL PEG surfaces (under cloud point) are comparable at values of $\sim$750, the natural period of oscillation (i.e., τ) is different for both systems (if both systems are considered critically damped, $\zeta = 1$, which is reasonable considering the shape of the frequency response) at $\sim$1 min for the 5 mg/mL system and at $\sim$4 min for the 1 mg/mL system. Interestingly, these time parameters correspond to the times to steady state for protein adsorption of Table 2, indicating a very probable relation between water structuring effects and protein adsorption.

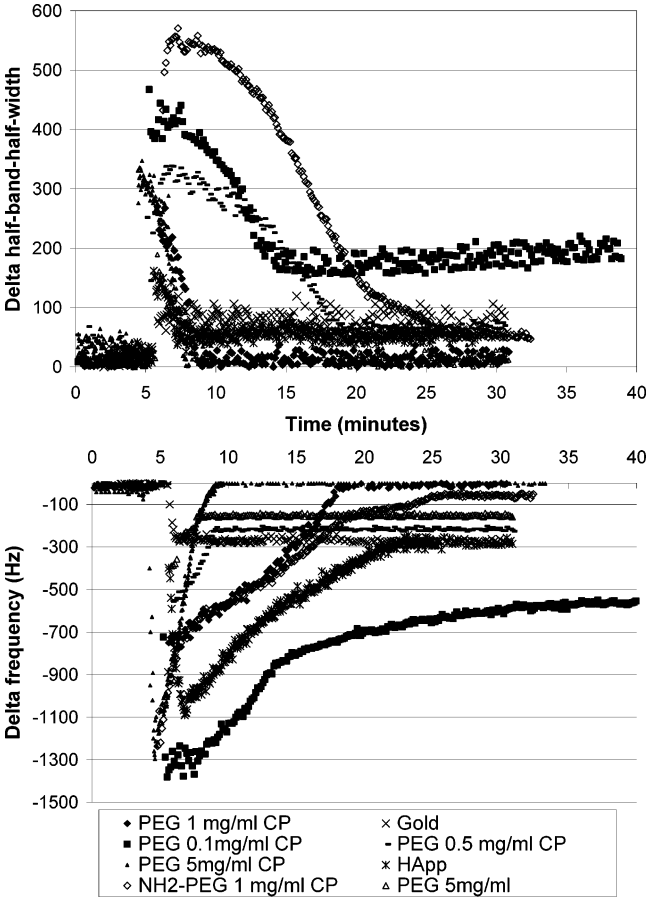

Figure 3. QCM dynamic data of protein adsorption on different PEG-covered surfaces; injection of the FBS solution at 5 min.

Thus, it can be worthwhile to inspect the dynamic response to protein adsorption of the different samples presented in Table 2. Figure 3 presents the dynamic recordings of the protein adsorption measurements.

The dynamic responses presented in Figure 3 are in good agreement with the hydration data of Figure 2. The response of PEG surfaces produced under non-cloud point conditions (represented in Figure 3 by the 5 mg/mL sample) is very rapid as the steady state is rapidly reached. The bare gold sample presents a similar dynamic behavior. However, all dynamic responses of the cloud point made PEG layers present a second-order-like dynamic response. Moreover, the steady-state gains relative to frequency for all these surfaces are comparable at a value of ~1100, and the time constants (the natural periods of oscillation) follow a similar pattern than for the hydration results of Figure 2 as the 1 mg/mL PEG surfaces (produced under cloud point) present a value of ~4 min while the 5 mg/mL PEG surfaces (produced under cloud point) present a value of 1 min. The 0.1 mg/mL PEG surfaces (produced under cloud point) present a 10 min time constant, but their gain is lower due to the large amount of protein molecules adsorbed on the layer. Once again, this is coherent with the large quantity of protein molecules that was found to be vibrating with the surface in Figure 2. It can probably be accepted that while PEG layers made with non-cloud point solvents repel, to some extent, protein adsorption mainly by steric forces, PEG layers made in Θ solvent achieve their anti-biofouling potential through a combination of steric forces and hydration/water structuring forces. Architecture of the PEG layers thus plays a large role in the resistance to protein adsorption, and this is exemplified by the 0.1 mg/mL PEG surfaces (produced under cloud point) which, although presenting more PEG molecules than all non-cloud point samples, adsorbs much more protein molecules.

Two PEG surfaces in Figure 3 present charges and create electrostatic interactions with the charged protein molecules. The heptylamine plasma layer is probably positively charged to some extent in the buffer media, and this can explain the second-order dynamic behavior to protein adsorption as negatively charged proteins can rapidly adsorb on the surface followed by the adsorption of other proteins with higher affinity to the surface (through the well-known Vroman effect) until a steady state is reached. The deprotected 1 mg/mL cloud point sample presents a similar behavior as positive charges on the amine PEG end group may also be present. In this case, the electrostatic effect is probably responsible for the increased lag of the dynamic response (i.e., time constant of ~6 min compared to 4 min for protected PEG) and for the large half-band-half-width variations compared to the protected sample.

The very large difference between the properties of PEG layers fabricated in water (i.e., good solvent) and PEG layers fabricated in a Θ solvent were foreseen based, as previously mentioned, on earlier reports. Indeed, part of the large differences observed might lie in the mechanical state of the PEG chains in the two different solvents. It has been known for a long time that PEG in aqueous solution do not behave as free rotating polymers as expected from the added flexibility of their ether linkages in water, but rather are "stiffened" by hydration so that their extension approaches that found in hydrocarbon polymers with hindered rotation.[24] The use of a Θ solvent completely modifies this forced mechanical state, allowing PEG molecules to present higher rotation freedom. Moreover, PEG molecules in a Θ solvent exhibit a higher thermodynamic affinity toward other PEG molecules than toward water, which is the opposite of the phenomenon observed in water, enabling PEG molecules to crowd on the reactive surfaces and yield dense layers. This behavior visibly allows an increase in PEG surface bonding through amine bounds and, although the surfaces are rinsed thoroughly after the reaction in good solvents such as water, may result in physisorbed PEG chains entrapped strongly in bound PEG chains.

3.3. Polymer Layer Mechanical Properties by QCM and AFM Measurements. The mechanical properties of the immobilized PEG molecules were characterized to get a better insight into the physical properties affecting protein adsorption and, ultimately, interactions with living cells. The QCM apparatus has been used to determine elastic compliance modulus of thin layers in viscoelastic systems (i.e., exhibiting energy losses linked to vibration). The elastic modulus can be isolated from QCM PEG grafting data (i.e., PEGylation), as the final frequency and half-band-half-width shifts measured at different harmonics were used in mathematical models previously validated with experimental data. The model used to calculate the elastic compliance of the different samples in this study was derived by Du and Johannsmann[25] and, for thin films in water, can be expressed as

$$\frac{\delta\Gamma}{-\delta f} \approx 2\pi n f_0 \eta J'_f \qquad (1)$$

where Γ is the half-band-half-width, f is the frequency (in Hz), n is the overtone order, f_0 is the reference frequency (5 MHz in our system), η is the viscosity of water (in Pa·s), and J'_f is the elastic compliance (in Pa^{-1}). By plotting the negative of the half-band-half-width shift divided by the frequency shift in function of the overtone order, one may determine from the

Table 3. QCM Results (δf and $\delta\Gamma$) of PEG Layers Immobilized on HApp-Activated Quartz Crystals for Different Experimental Conditions[a]

surface	av freq shift (Hz)	Sauerbrey PEG mass (ng/mm^2)	PEG surface density (chains/nm^2)	av half-band-half-width shift	elastic compliance (GPa^{-1})
PEG 0.1 mg/mL CP	-270 ± 20	1.0 ± 0.2	0.2	940 ± 60	19 ± 3
PEG 1 mg/mL CP	-1400 ± 60	4.9 ± 0.3	0.9	480 ± 30	1.9 ± 0.3
PEG 5 mg/mL CP	-1150 ± 80	4.0 ± 0.2	0.7	500 ± 40	2.1 ± 0.3
PEG 0.1 mg/mL	-250 ± 40	0.9 ± 0.3	0.15	200 ± 40	2.4 ± 0.4
PEG 1 mg/mL	-310 ± 20	1.1 ± 0.2	0.2	230 ± 30	2.2 ± 0.3
PEG 5 mg/mL	-340 ± 30	1.2 ± 0.2	0.2	230 ± 20	2.1 ± 0.2

[a] Calculated Sauerbrey mass, surface density from Sauerbrey mass, and elastic compliance modulus are also presented.

slope of the graph the elastic compliance of the thin film. The PEGylation results are reported in Table 3.

The reported frequencies and half-band-half-widths are those obtained following repeated rinsing in water. It is to be noted that the surface density reported in Table 3 is simply calculated by converting the mass determined by the Sauerbrey equation using the molecular weight of the PEG polymer.

The calculated polymer Sauerbrey mass immobilized on the crystals and the surface density calculated from the Sauerbrey mass presented in Table 3 should be taken with great care as, like previously discussed, viscoeleastic systems cannot be modeled accurately with the Sauerbrey model. Large viscoelastic energy losses are indeed known to decrease observed absolute frequency shifts. However, an order of magnitude can be observed, which is coherent with the XPS data of Table 1. Again, PEG surfaces fabricated under cloud point show a larger number of PEG molecules on their surface compared to non-cloud point samples. Maximal PEG density is achieved at cloud point sample 1 mg/mL. The elastic compliance of the thin films indicates a rather rigid behavior except for, interestingly, the 0.1 mg/mL PEG CP sample, which elastic compliance is 9 times that of the other samples. It should be recalled that the elastic compliance is the inverse of the real part of the shear modulus, so that a high elastic compliance indicates a "softer" material. The architecture of this sample is definitively very different to that of the other samples, a fact that was foreseen by the extremely high protein adsorption of these PEG layers. It should be noted that these measurements were made in water, and it could be worthwhile to eventually study the elastic behavior of the layers in solvents with varied osmotic properties as this could have an important impact on the architecture of the layers and, thus, on the values of the elastic compliance.

The AFM can also be used to get information on the mechanical properties of the polymer layers, specifically the colloidal probe force measurement method previously described.[22] In this technique, a relatively large sphere (i.e., diameter of 4.1 μm) glued to a cantilever is approached to the surface and is used to fully compress the polymer layer before retracting. The cantilever deflection is recorded and translated into force values relative to the diameter of the sphere. The results of such measurements in water and in a 300 mOsm RPMI 1640 buffer are reported in Figure 4 for different PEG samples.

The AFM compression force curves of Figure 4 show that the hydrated PEG layers have a "thickness" of 4−8 nm in RPMI buffer, the thickest films exhibited by the cloud point-fabricated samples, while the 0.1 mg/mL non-cloud point was the thinnest. By thickness, here, we mean the separation distance at which the force between the colloidal probe and the PEG surfaces became nonnil when approaching the cantilever toward the surfaces. All PEG samples produced under cloud point have similar compression profiles while the non-cloud point samples have decreased compression resistance and thickness from highest to lowest concentrations. The AFM compression data in water in the same figure show the electrostatic effects of the

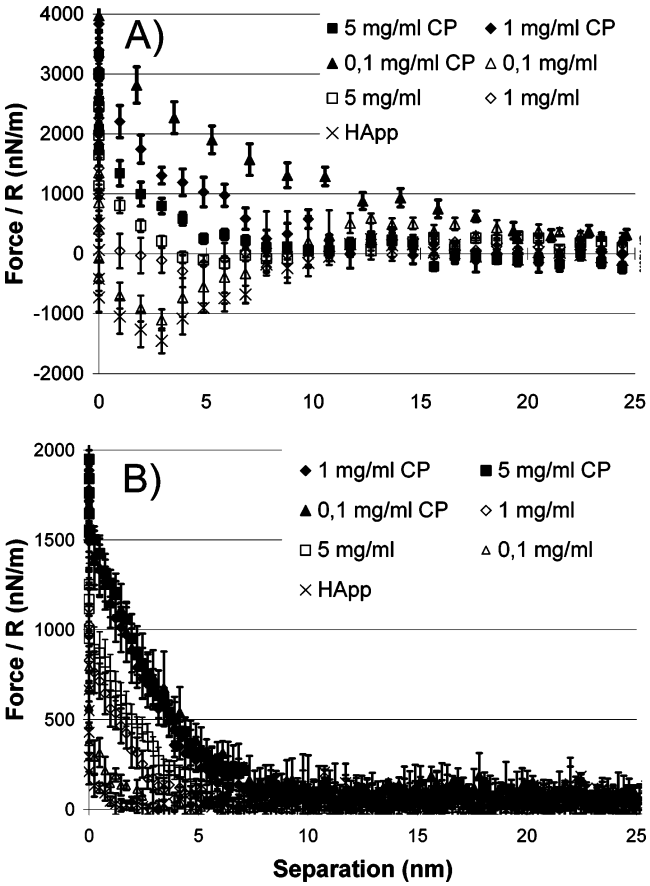

Figure 4. Compression AFM force curves using the colloidal probe method for different PEG samples in water (A) and in RPMI buffer (B).

negatively charged AFM silica sphere and the positively charged plasma layer for the samples with small PEG densities, i.e., for non-cloud point PEG samples 1 and 0.1 mg/mL, as a "jump to contact" was recorded upon approach of the surface. This probably translates into a poor coverage of the entire surface for these two conditions, which is coherent with XPS data of Table 1 and protein adsorption experiments. 5 mg/mL PEG surfaces produced under cloud point show similar behavior to compression in water and in buffer, but the 1 mg/mL and, principally, the 0.1 mg/mL PEG surfaces produced under cloud point both present a significant increase of their thickness, while their resistance to compression (i.e., the slope of the compression curve) is slightly reduced. The use of a better solvent and the high degree of freedom of their architecture probably enable the extension of the polymer chains in the solvent, a result that was not expected and not previously reported. Evidence builds up on the unusual architectures of the layers made under cloud point conditions and their extreme sensitivity to PEG concentration on the final PEG layer characteristics. Further testing would be required to assess the behavior of the cloud point samples in intermediate solvent osmolarities.

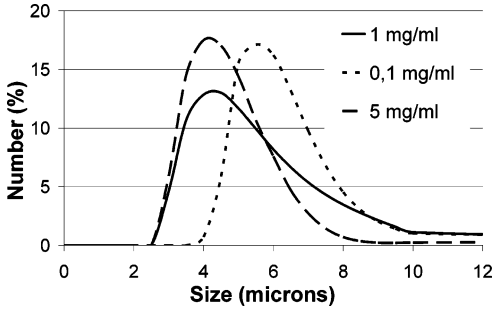

Figure 5. Size distribution of PEG agglomerates in Θ solvent in number percent. The size distributions shown were stable over time (i.e., from injection to end of experiment) for all PEG concentrations.

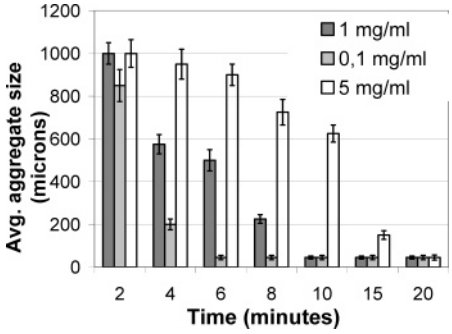

Figure 6. Mean PEG aggregate size in Θ solvent in volume percent as a function of time.

3.4. Agglomeration Kinetics of PEG Molecules in Θ Solvent. The very wide range of characteristics (i.e., number of bound PEG molecules, resistance to protein adsorption and mechanical properties) exhibited by the PEG surfaces produced under cloud point at different PEG concentrations is not coherent with the traditional Alexander and de Gennes models, contrarily to the PEG surfaces fabricated in water. In a Θ solvent, PEG molecules are known to form large aggregates of different size distributions depending on a variety of factors such as concentration, shear stress, and temperature.[23] Using a light diffraction-based instrument, the Malvern Mastersizer, the size of the polymer aggregates was measured over time to assess possible effects of PEG agglomerate size in solution on final PEG layer chemistry and properties. To conduct such measurements, PEG is usually injected from a concentrated well-mixed PEG aqueous solution to the instrument in which is circulated the Θ solvent to achieve desired PEG concentration and to monitor the agglomeration process. However, the PEG molecules in our study display a relatively short stability in aqueous environments, owing to the hydrolysis of the active ester reactive groups available on one end of the PEG polymers. This hydrolysis is complete in approximately an hour at room temperature and is obviously much faster at higher temperatures, thus the rationale to use Na_2SO_4 in this system to achieve cloud point conditions at room temperature. The time necessary to achieve the dissolution of the solid PEG has to be reduced to a minimum by hand agitation. Typically, an agitation of 2 min is required to ensure dissolution of visible solid PEG particles and proceed with the surface immobilization reaction. For the light diffraction measurements, PEG was dissolved for 2 min by hand agitation and added directly to the Θ solvent circulating in the apparatus to mimic as closely as possible the actual procedure for PEG immobilization. The agitation in the apparatus was also set to be as close as possible to the agitation present in typical immobilization reactions. The results in number percent are presented in Figure 5, and the size of the agglomerates in volume percent over time is presented in Figure 6.

Figure 5 indicates that, in terms of number percent, the PEG aggregate size is constant throughout the surface immobilization reaction. Lowering the PEG concentration tends to yield larger polymer aggregates in solution, with a 50% difference between the 0.1 and 5 mg/mL cases. This could perhaps be explained by the smaller number of aggregates for the lower concentrations inducing fewer collisions with the impeller providing the shear stress in the apparatus. PEG molecules may have more time to agglomerate before being submitted to the shear stress of the apparatus at lower concentrations. On the other hand, the PEG aggregate sizes in terms of volume percent were shown to vary importantly with time for all PEG concentrations. Indeed, Figure 6 clearly shows that very large PEG aggregates are present in the system and that the kinetics of large aggregates formation are principally controlled by a homogenization/dissolution process. When placed in the Θ solvent, solid PEG initially forms very large aggregates (which can be at some times multimodal in their size distribution), which are then homogenized by the shear stress provided by the impeller in the apparatus and the gradual dissolution of the PEG molecules. Interestingly, the steady state is reached with very different speeds depending on the PEG concentration. For example, a surface reaction at cloud point with a PEG concentration of 5 mg/mL will occur mainly between the surface and agglomerates larger than 600 μm for the first 10 min of the reaction. On the other hand, the same 10 min of the reaction will mainly occur between aggregates of 50 μm and the surface for a PEG concentration of 0.1 mg/mL, which is an order of magnitude difference with the 5 mg/mL PEG solution. The kinetic behavior of the agglomerates in the Θ solvent can perhaps begin to explain the very different architectures observed previously.

3.5. Chemical Bonding Properties of the Deprotected PEG Layers. The immobilized PEG layer system studied in this article allows the covalent immobilization of molecules after Boc deprotection of the PEG molecules exposing primary amino groups. Moreover, the molecules can be immobilized in a spatially defined manner by using a dispensing robot. The wide range of polymer architecture expressed by the different PEG samples studied makes it important to monitor the chemical grafting potential of the different samples. A fluorescent molecule, carboxyfluorescein (CF), was deposited by a dispensing robot on the different samples and immobilized by a covalent amide bound. The fluorescence intensity, after rinsing, is indicative of the quantity of CF molecule that successfully bound to the PEG-end amines if the concentrations of CF used are located in the linear nonquenching regime. This was ensured by a calibration curve done on different samples (data not shown). The results of the immobilization of CF are shown in Figure 7.

Figure 7 shows that all samples covalently bind CF molecules as the signals of the covalently immobilized CF were always stronger than those of the adsorbed CF for a given PEG sample. However, the sample which was the most resistant to protein adsorption, 5 mg/mL produced under cloud point, also presents less accessible amine end groups for chemical grafting than all the other samples. This could be caused by the steric hindrance of the well-packed PEG chains. The samples made from 2.5 mg/mL PEG under cloud point and lower PEG concentrations all show similar chemical availability of the amine end groups for CF immobilization, except for the 0.1 mg/mL sample, which exhibits nonhomogeneous fluorescence that could be due to CF molecules trapped in the PEG layer architecture. This hypothesis seems to be confirmed by an increase in the nonspecific adsorption of CF molecules on the samples. As observed from

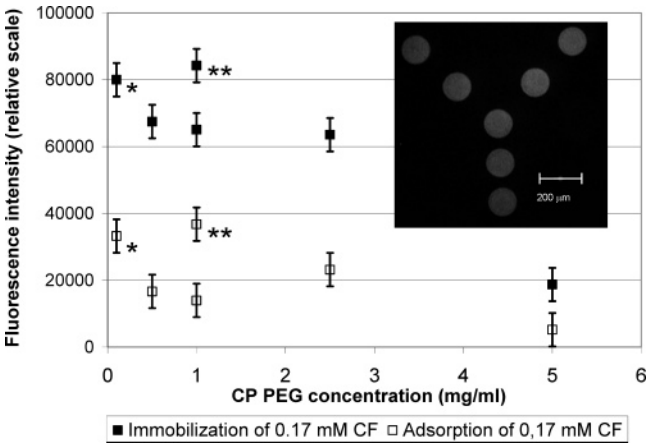

Figure 7. Fluorescence intensity measured from covalently bound CF fluorescence intensity and adsorbed CF for different PEG layers. * indicates nonhomogeneous fluorescence, ** indicates non-cloud point sample and nonhomogeneous fluorescence. Inset shows a typical CF geometrical design immobilized on a 1 mg/mL PEG sample produced under cloud point.

QCM data, the 0.1 mg/mL PEG sample was also the sample which was the most prone to protein adsorption. The behavior of the samples fabricated under non-cloud point conditions is for all concentrations similar to that of the 0.1 mg/mL cloud point sample. Nonhomogeneous fluorescence is also observed with an increase in CF adsorption. However, the behavior of samples fabricated under non-cloud point conditions could be explained by the nonhomogeneous coverage of the surfaces by PEG molecules that was observed by AFM force measurements in water or by the low surface PEG chain density that was observed by XPS. Thus, all the layers could be used to graft covalently and spatially molecules with varying yields, which depend on the underlying PEG surfaces.

4. Conclusion

A system to immobilize PEG molecules on various solid substrates was described, and the use of two reaction parameters, i.e., (1) the use of a Θ solvent and (2) different polymer concentrations in solution, was studied to assess their impact on PEG layer properties. Results show that PEG layers deposited using cloud point conditions present unusual reaction PEG concentration-dependent architectures as observed, noticeably, by protein adsorption assays and AFM force measurements. While high polymer concentrations yield structurally stiff layers, low PEG concentrations exhibit higher structural flexibility which enhances chemical bonding capabilities but, on the other hand, can enhance nonspecific protein adsorption. Traditional models do not represent well the observed immobilized PEG polymer structures on the surfaces. The size of polymer aggregates in a Θ solvent during a surface reaction may play an important role in final layer properties as PEG aggregation kinetics showed important variations in aggregate sizes for different PEG concentrations, which correlate with observed mechanical and physicochemical layer properties. It is not yet known what responses these architectures will trigger when exposed, for example, to live cells. This is the aim of a future work in our laboratory.

Acknowledgment. This work was supported by the Canadian Foundation for Innovation through an On-going New Opportunities Fund (project # 7918) and by the Université de Sherbrooke. We thank the National Science and Engineering Research Council of Canada (NSERC) for financial support through Canada Graduate Scholarship (CGS) awarded to Yves Martin.

References and Notes

(1) Vermette, P.; Meagher, L. *Colloids Surf., B* **2003**, *28*, 153−98.
(2) Alexander, S. *J. Phys. (Paris)* **1977**, *38*, 983−7.
(3) de Gennes, P. G. *J. Phys. (Paris)* **1976**, *37*, 1445−52.
(4) Harder, P.; Grunze, M.; Dahint, R.; Whitesides, G. M.; Laibinis, P. E. *J. Phys. Chem. B* **1998**, *102*, 426−36.
(5) Pasche, S.; Voros, J.; Griesser, H. J.; Spencer, N. D.; Textor, M. *J. Phys. Chem. B* **2005**, *109*, 17545−52.
(6) Drobek, T.; Spencer, N. D.; Heuberger, M. *Macromolecules* **2005**, *38*, 5254−9.
(7) Fick, J.; Steitz, R.; Leiner, V.; Tokumitsu, S.; Himmelhaus, M.; Grunze, M. *Langmuir* **2004**, *20*, 3848−53.
(8) Kingshott, P.; McArthur, S.; Thissen, H.; Castner, D. G.; Griesser, H. J. *Biomaterials* **2002**, *23*, 4775−85.
(9) Unsworth, L. D.; Tun, Z.; Sheardown, H.; Brash, J. L. *J. Colloid Interface Sci.* **2005**, *281*, 112−21.
(10) Vladkova, T.; Krasteva, N.; Kostadinova, A.; Altankov, G. *J. Biomater. Sci., Polym. Ed.* **1999**, *10*, 609−20.
(11) Golander, C.; Herron, J.; Lim, K.; Claesson, P.; Stenius, P.; Andrade, J. In *Poly(ethylene glycol) Chemistry, Biotechnical and Biomedical Applications*; Harris, J., Ed.; Plenum Press: New York, 1992; pp 221−245.
(12) Kingshott, P.; Thissen, H.; Griesser, H. J. *Biomaterials* **2002**, *23*, 2043−56.
(13) Unsworth, L. D.; Sheardown, H.; Brash, J. L. *Biomaterials* **2005**, *26*, 5927−33.
(14) Piehler, J.; Brecht, A.; Valiokas, R.; Liedberg, B.; Gauglitz, G. *Biosens. Bioelectron.* **2000**, *15*, 473−81.
(15) Thissen, H.; Johnson, G.; Hartley, P. G.; Kingshott, P.; Griesser, H. J. *Biomaterials* **2006**, *27*, 35−43.
(16) Hansson, K. M.; Tosatti, S.; Isaksson, J.; Wettero, J.; Textor, M.; Lindahl, T. L.; Tengvall, P. *Biomaterials* **2005**, *26*, 861−72.
(17) Li, N.; Tourovskaia, A.; Folch, A. *Crit. Rev. Biomed. Eng.* **2003**, *31*, 423−88.
(18) Griesser, H. J. *Vacuum* **1989**, *39*, 485−8.
(19) Vermette, P.; Gengenbach, T.; Divisekera, U.; Kambouris, P. A.; Griesser, H. J.; Meagher, L. *J. Colloid Interface Sci.* **2003**, *259*, 13−26.
(20) Vermette, P.; Griesser, H. J.; Kambouris, P.; Meagher, L. *Biomacromolecules* **2004**, *5*, 1496−502.
(21) Cleveland, J. P.; Manne, S.; Bocek, D.; Hansma, P. K. *Rev. Sci. Instrum.* **1993**, *64*, 403−5.
(22) Ducker, W. A.; Senden, T. J.; Pashley, R. M. *Langmuir* **1992**, *8*, 1831−6.
(23) Pang, P.; Englezos, P. *Colloids Surf., A* **2002**, *204*, 23−30.
(24) Bailey, F.; Callard, R. *J. Appl. Polym. Sci.* **1959**, *1*, 56−62.
(25) Du, B. Y.; Johannsmann, D. *Langmuir* **2004**, *20*, 2809−12.

MA060921F